Final Draft
of the original manuscript:

Anders, I.; Rockel, B.:
The influence of prescribed soil type distribution on the representation of present climate in a regional climate model
In: Climate Dynamics (2008) Springer

DOI: 10.1007/s00382-008-0470-y

Noname manuscript No.
(will be inserted by the editor)

The influence of prescribed soil type distribution on the representation of present climate in a regional climate model

Ivonne Anders · Burkhardt Rockel

Received: date / Accepted: date

Abstract Two model simulations with the regional climate model CLM performed with different prescribed soil type distributions are analysed to investigate consistent dry and warm biases during summer in south-eastern Europe evident in a variety of regional climate models (RCMs). The conventional soil type distribution defines sandy loam in the southeast of Europe; whereas the modified one defines a large area of silt loam instead. As a consequence of the different soil characteristics, the results indicate increased soil moisture in the modified simulation compared to the control simulation. In addition to local changes in near surface parameters, large-scale changes involving temperature, precipitation and surface pressure are observed. Some corrections of the temperature bias in southeastern Europe are obtained with the prescription of the different soil type, though significant model biases remain in this region.

Keywords soil moisture · regional climate modelling · summer drying

1 Introduction

Previous simulations over Europe carried out with different regional climate models (RCMs) show a dry and warm bias to the north and east of the Black Sea during summer (*Jacob et al.* (2007), *Hagemann et al.* (2004), *Moberg and Jones* (2004), *Räisänen et al.* (2004), *Vidale et al.* (2003), *Noguer et al.* (1998), *Christensen et al.* (1997)). As the results from RCM climate simulations are not only used by regional climate modellers, but also by scientists in other disciplines, this so called "summer drying" presents a major issue affecting a larger scientific community.

I. Anders
Institute of Coastal Reserach, Regional Atmospheric Modelling Group, GKSS Research Center, Max-Planck-Str.1, D-21502 Geesthacht, Germany.
Tel.: +49-4152-871854
Fax: +49-4152-8741854
E-mail: ivonne.anders@gkss.de

B. Rockel
Institute of Coastal Reserach, Regional Atmospheric Modeling Group, GKSS Research Center, Max-Planck-Str.1, D-21502 Geesthacht, Germany.

Approaches to explain the phenomena of summer drying have been undertaken by, for example, *Machenhauer et al.* (1998) putting forward systematic dynamical errors of the driving model and the RCM. However, deficiencies in physical parameterization and in land surface parameter fields could be possible reasons as well (*Hagemann et al.* (2001)). *Seneviratne et al.* (2006a) investigated the influence of soil moisture-coupling for recent and future climate conditions in a regional climate model. They showed that the coupling can strongly affect the temperature variability e.g. in the Mediterranean for the present climate and Central and Eastern Europe for the future climate. In another study *Rowell and Jones* (2006) defined the causes of the future European summer drying and assessed the uncertainties respectively. *Fischer et al.* (2007a,b) presented an analysis of the 2003 European summer heat wave including the associated land-atmosphere interactions involved. They pointed out that the available soil moisture content during spring is very important in order to get a realistic simulation of the observed climate during the subsequent summer in this region. Furthermore, the models sensitivity of initial soil moisture conditions on the European heatwave 2003 has been investigated by *Ferranti and Viterbo* (2006).
Soil moisture plays an important role within the climate system because it has a long memory that influences the atmospheric processes at the land surface (*Seneviratne et al.* (2006b), *Pan et al.* (2001), *Koster and Suarez* (2001), *Seneviratne et al.* (2006b), *Wu and Dickinson* (2004)). Varying soil moisture has a direct influence on soil temperature, evaporation and surface albedo (*Eltahir* (1998)). Thereby radiation and humidity conditions at surface level change. *Findell and Eltahir* (2003a,b) investigated the interaction between soil moisture and the boundary layer. They showed that the variability of soil moisture conditions over large regions has a direct influence on important processes associated with rainfall in the boundary layer. The positive feedback between soil moisture and precipitation rate is supported by studies from *Schär et al.* (1999), *Eltahir* (1998) and *Betts et al.* (1996). *Koster and Suarez* (2003) pointed out that a significant impact on precipitation strongly depends on the initial soil moisture and the sensitivity of evaporation on the soil moisture state. *Betts* (2004) found the strong evaporation-precipitation feedback over the continents of the Northern Hemisphere during summer in the ERA40-model. This is supported by *Koster et al.* (2004) and *Koster et al.* (2006) identifying different regions on the continent with a strong coupling between soil moisture and precipitation. The influence of changing soil moisture conditions on the surface albedo can be masked by the strong response of the vegetation to water stress (*Teuling and Seneviratne* (2008)).
The natural soil moisture field is characterized by small-scale spatial and temporal variability affected by a complex orography and spatially variable vegetation as well as soil type distribution. These components can only be schematically implemented in RCMs. Several investigations have been carried out focusing on the sensitivity of RCMs to changes in vegetation and/or land use (e.g. *Sánchez et al.* (2007), *Marshall et al.* (2004), *Pielke* (2001), *Pielke et al.* (1999)). The soil types in RCMs have different fixed definitions for soil characteristics such as porosity, heat capacity and water conductivity. Such parameters strongly influence the soil moisture conditions and surface fluxes. *Block* (2007) identified the uncertainty for simulated surface variables by varying the values of these soil characteristics in the CLM within a reasonable range. A strong response was seen in the Mediterranean and the southeast of Europe in latent and sensible heat fluxes and in the air temperature. *Fennessy and Shukla* (1999) identified the impact of initial soil moisture as mainly local and being largest on the near-surface fields.

The majority of RCMs use a soil type distribution derived from a global dataset provided by the Food and Agriculture Organization (FAO) (see chapter 2.2). For the southeast of Europe - the region of the summer drying phenomena seen in RCMs - from FAO soil map the soil type sandy loam is derived. However, the International Soil Map of Europe published by *Stremme* (1937) identifies silt loam. The occurrence of silt loam in this area is supported by a dataset recently published by *Haase et al.* (2007).
In this study we have investigated the influence of the two described soil type distributions on a RCMs representation of present climate. Our main focus has been on changes due to different soil characteristics in south-eastern Europe.

2 CLM regional climate model and experimental model setup

2.1 Model details

The Climate Local Model (CLM) is the climate version of the weather forecast model of the German Weather Service (DWD) (*Böhm et al.* (2006)). It is a non-hydrostatic RCM, using a regular latitude/longitude grid with a rotated pole and a terrain following height coordinate. The CLM includes the multilayer soil model TERRA (*Schrodin and Heise* (2001)). The evapotranspiration of plants is parameterized based on the Biosphere-Atmosphere Transfer Scheme (BATS) (*Dickinson et al.* (1986)). The parameterization of bare soil evaporation follows *Dickinson* (1984). In the TERRA soil model ten active layers for energy transport (up to a depth 15 m) are used. The bottom layer (10th layer from 7.66 m to 15.34 m depth) is the so called *climate layer*, where the annual mean temperature is prescribed as a boundary value (*Doms et al.* (2002)). For the hydrological section the same layers as in the thermal section are set, but only to a depth of around 4 m (8 layers). At the bottom boundary of the 8th layer only the downward gravitational transport is considered and capillary transport is neglected (*Doms et al.* (2002)). According to the soil type distribution the soil moisture is initialised at the beginning of the simulation by the forcing data and evolves freely without any correction or nudging by the driving data in the course of the simulation. The model has been used previously for the simulation of present and/or future climate conditions in the EU funded projects: PRUDENCE (http://prudence.dmi.dk/), ENSEMBLES (http://ensembles-eu.org/) and also in the *klimazwei* project funded by the German government (http://www.klimazwei.de/ and http://sga.wdc-climate.de). For this investigation the model version 3.21 is used which is a pre-version of the CCLM4 (a merged version of COSMO-LM and the climate version CLM). It was validated in detail by *Jaeger et al.* (2008).

2.2 Gridded geographical distribution of soil type fields

RCMs usually include soil types derived from the FAO global soil map. The FAO developed an international standardized classification to describe soil characteristics (for details see *Soil Map of the World* (*FAO/UNESCO* (1974))). For climate modellers a gridded version known as *Digital Soil Map* of the World (DSMW) (*FAO* (1996)), with a spatial resolution of 5' by 5' (approx. 9 km x 9 km) is available. It contains the DSMW map and derived soil properties such as soil depth, soil moisture storage capacity and

soil drainage class.
For the regional scale we selected the *International soil map of Europe* published by *Stremme* (1937) with a scale of 1:2 500 000. This map contains eleven soil texture classes and two mixed classes and has been digitized and classified for areas of silt loam. We added these areas to the FAO soil distribution map and used it as the second soil type distribution within our experiment (see the following section).

Table 1 Selection of hydraulic and thermal parameters of sandy loam (*Doms et al.* (2002)) and silt loam (estimated from *Driessen* (1986), *Doms et al.* (2002))

	sandy loam	silt loam
volume of voids [-]	0.445	0.485
field capacity [-]	0.260	0.360
permanent wilting point [-]	0.100	0.130
heat capacity $[10^6 J/(m^3 K)]$	1.350	1.450
heat conductivity $[W/(Km)]$	1.74	1.25
fraction of sand [%]	65	10
fraction of clay [%]	10	15

2.3 Experimental design and observational data

The model domain covers Europe with a spatial resolution of 50 km and 32 vertical levels for the atmosphere. The pole of the rotated model grid is located at 50.75° N and 18° E (cf. Figure 1 excludes the sponge zone). The simulations are driven by NCEP/NCAR re-analysis data (*Kalnay et al.* (1996)). In addition to the forcing at the lateral boundaries (*Davies* (1976)) a spectral nudging technique as described by *Feser and von Storch* (2005) has been applied. The soil type distribution used in RCMs is derived from FAO soil textures. The original three fractions (coarse, medium and fine) have been mapped to base porosities used in the model. After interpolation these mixed values have been assigned to the model used five standard soil types (sand, sandy loam, loam, loamy clay and clay) according to the individual porosity values in the models look-up table for the soil characteristics. Further surface properties include the definition of ice, rock and sea water. Due to this method the derived distribution can deviate from distributions used by other RCMs.
We have performed two 13-year CLM simulations covering the period 1993-2005. The simulations were initialized on January 1^{st}, 1989, allowing a four year spin-up time to reduce the influence of the initial soil moisture. One simulation has used the soil type distribution derived from the FAO dataset (hereafter referred to as the control simulation (CTL)). In the second simulation we used the same soil type distribution as for the control simulation but with areas of silt loam from the *International soil map of Europe* (hereafter referred to as the modified simulation (MOD)). The areas of silt loam are not included in the FAO soil map, but other sources (e.g. *Haase et al.* (2007)) support the occurrence of silt loam. The associated soil parameters are listed in Table 1. For comparison of the modelling results the global high-resolution gridded temperature and precipitation data set CRU TS2.1 (*Mitchell and Jones* (2005)) has been used. This data set with a spatial resolution of 0.5°x0.5° covers the time period

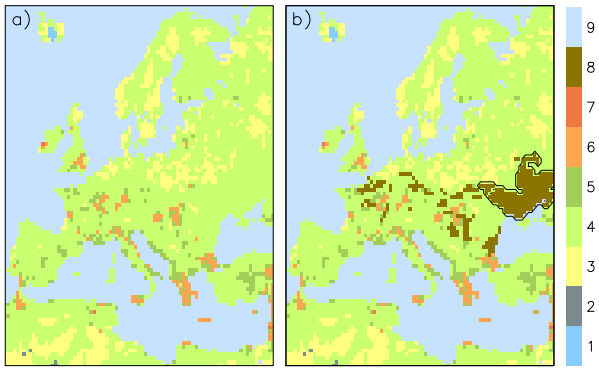

Fig. 1 Soil type distribution derived from (a) FAO and (b) the same as a) but with silt loam areas added from the International Soil Map of Europe (1 - ice, 2 - rock, 3 - sand, 4 - sandy loam, 5 - loam, 6 - loamy clay, 7 - clay, 8 - silt loam, 9 - sea water). Black contour indicates the area of interest (cf. Figures 3, 4, 5, 7, and 6 and Chapter 3.2)

1901-2002 and is based on in-situ measurements from a large number of stations.

3 Results

3.1 Validation of control simulation

To validate the control simulation we compared a 10-year simulation period 1993-2002 with the CRU dataset for the same period. Monthly and seasonal correlations and biases for air temperature and precipitation have been analysed.
Correlations between modelled and observed temperature and precipitation are high with values around r≅0.85. During summer the correlation is lower (r≅0.5-0.85) for the Carpathian Mountains, parts of the Iberian Peninsula and southeast parts of the Mediterranean. Previous investigations have also shown a pronounced negative bias of up to -3 K during spring in the north and northeast of Europe (not shown). A reason explaining this phenomenon is related to a higher number of simulated snow-days in March, April and May. Over south-eastern Europe an overestimation of air temperature during summer of up to 3 K (see Figure 2) is evident together with a pronounced underestimation of precipitation (of up to up to -25 mm) which extends into the northern Mediterranean region. This is about 50 % of the precipitation in this season. The positive temperature bias and negative precipitation bias reflect the commonly known phenomena of summer drying seen in RCMs (e.g. *Jacob et al.* (2007), *Hagemann et al.* (2004) and *Noguer et al.* (1998)). The used model version has been validated in more detail by *Jaeger et al.* (2008).

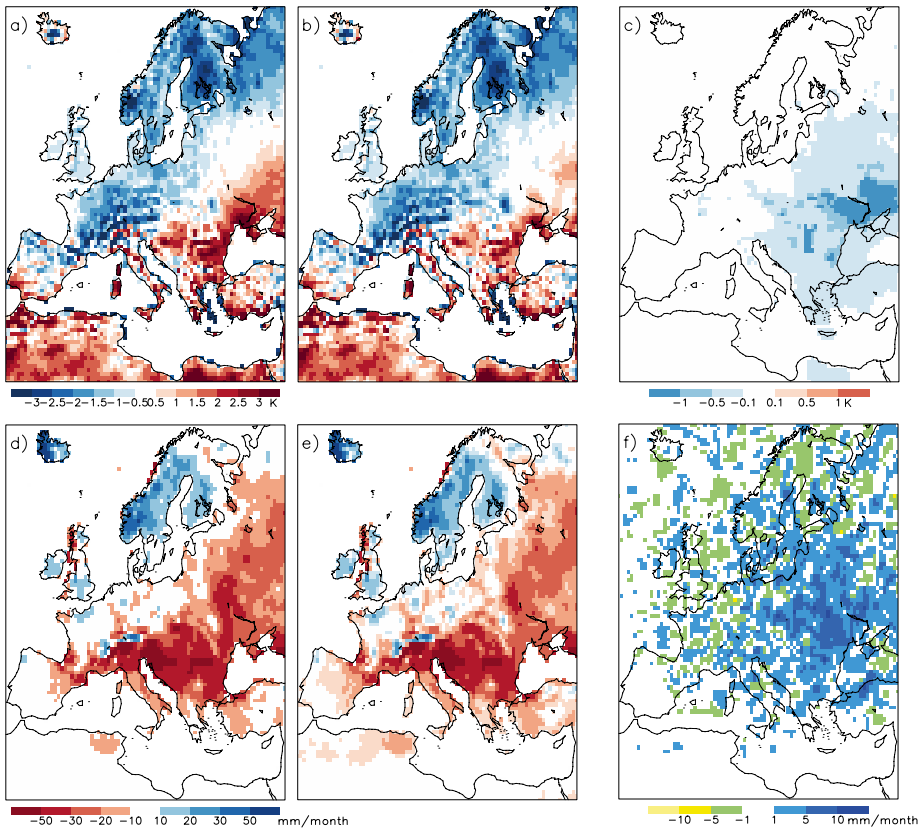

Fig. 2 Top row: Bias of mean 2m-temperature over time period June-August compared to CRU data for the a) control simulation and b) modified simulation. c) difference between both simulations (MOD-CTL), Bottom row: Bias of mean precipitation over the time period June-August compared to CRU data for the d) control simulation and e) modified simulation. f) difference between both simulations (MOD-CTL).

3.2 RCM response on changing soil conditions

Based on the results of using different soil characteristic definitions (cf. Table 1), areas of silt loam in the modified simulation are initialized with a 9 % higher soil moisture in all active soil layers compared to the control simulation using sandy loam. After initialisation soil moisture develops freely without any correction or nudging during the simulation. Figure 3-a) shows the mean annual cycles of soil moisture in all layers affected by the roots. Due to a mean root depth in this area of about 1.5 m, the upper seven soil layers are taken into account in these plots. The differences between both simulations can be seen in Figure 3-b) as the change MOD-CTL in relation to the amount which is available in the CTL simulation. The values are spatial averages over the connected silt loam area north of the Black Sea (cf. Figure 1-b)) over the time period 1993-2005. During the whole simulation period using silt loam higher available soil moisture is observed in all active soil layers in the modified simulation. The upper four layers show a similar pattern with about 10-15 % more soil moisture during spring,

autumn and winter and values up to 30 % during summer. The lower layers show values even of up to 75 % during spring time, which coincides with the annual maximum of moisture in all soil layers. In MOD a strong annual cycle of soil moisture is discernible in the lower soil layers (from the 5th layer downward). In the CTL simulation there is no annual cycle in the soil moisture for the soil layers 7 to 10 (the most bottom). This can be traced back to the assumption that due to small values for the saturation of the soil in this area there is not enough moisture available in the model to fill the lower soil layers. Figure 7 shows the temporal evolution of the available soil moisture in the root zone as percentage of the saturation. As the soil in both simulations is not at saturation it shows a constant increase of the values of about 10 % over the whole year in MOD (cf. Table 2 for exact values). The Figures 8-g) and -h) show that this effect is limited to the silt loam area.

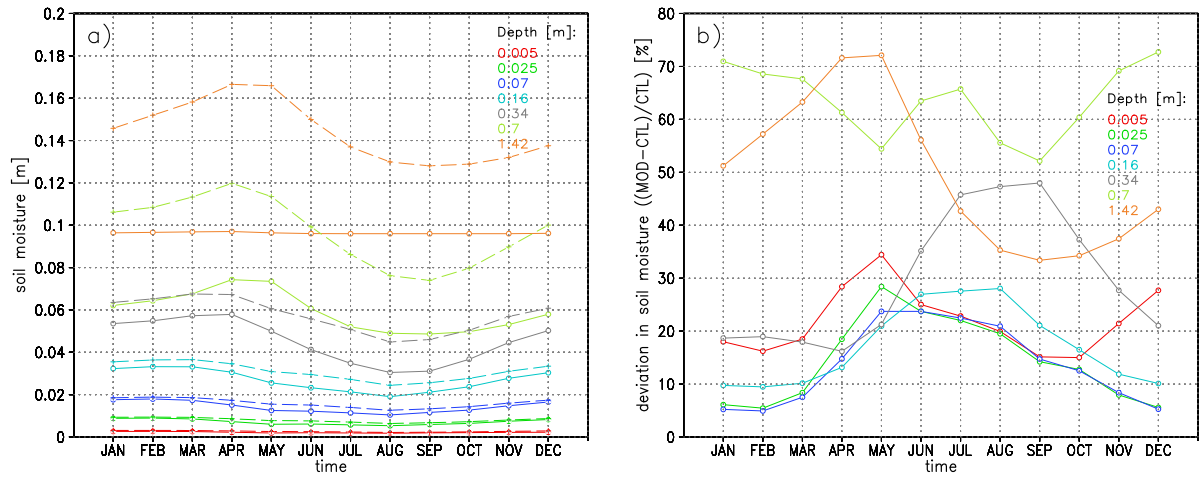

Fig. 3 Mean annual cycle of soil moisture for all soil layers affected by the roots a) for CTL simulation (solid) and MOD simulation (dashed) and b) as the difference between MOD and CTL as the relation (MOD-CTL)/CTL and as the mean over the connected silt loam area north of the Black Sea (cf. Figure 1). The numbers indicate the mean depth of each soil layer, measured from the earth's surface.

Physical considerations explaining the differences in surface properties are related to increased soil moisture which leads to increased net solar radiation. The latter is due to a decrease in albedo (not shown) which increases the absorption of radiation at the surface. This effect is accompanied by a decrease of both surface temperature and hence, terrestrial outgoing radiation because more energy is used for evaporation. This decrease in the albedo is small with values about 1 to 3 % in April and May and less than 1 % during summer. This can be explained by the generally small values for soil moisture in these months, so that the increasing soil moisture has not a very big effect on the surface albedo. Further the decrease of surface albedo due to increasing soil moisture is masked by the large influence of the vegetation state. *Teuling and*

Seneviratne (2008) investigated the dynamic of surface albedo and refered to the strong spectral response of vegetation to water stress. This agrees with results from *Zaitchik et al.* (2007).

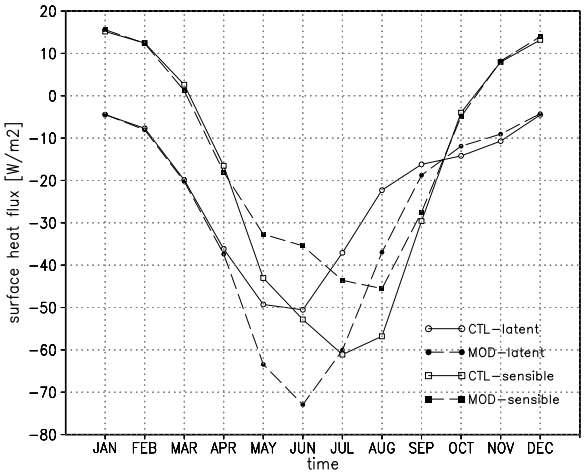

Fig. 4 Temporal evolution of latent heat flux (circles) and sensible heat flux (squares) at surface. The values for CTL (solid) and MOD (dashed) integrations are spatially averaged over the connected silt loam area north of the Black Sea (cf. Figure 1) .

Figure 4 shows the annual cycle of the surface latent heat flux. From May until August up to 60 % higher values for evaporation occur. Where e.g. in CTL in July an evaporation rate of -1.28 mm/day can be observed in MOD it is increased by -0.8 mm/day (see also Table 2). The changes in the heat fluxes are spatially limited on the grid points with the silt loam definition (cf. Figure 8-d) and -e)).
The influence of higher soil moisture is also clearly reflected in the soil temperatures. Figure 5-a) shows the mean annual cycle of the soil layers temperatures in the root zone for each simulation. Independent from model integrations the thicknesses of the upper layers is very small and is increased to the soil depth. Hence the amplitude of the temperature of the upper soil layers is very similar and the annual maximum occurs at about the same time in late July/beginning of August. According to the heat transfer we can clearly identify the typical lagged temperature response from the surface to the deep soil layers. Due to the in general higher soil moisture conditions in MOD the amplitude of the soil layers temperature is reduced by up to 2.5 K compared to the CTL simulation. Hence, we find a weaker annual cycle of soil temperature in the modified simulation results. In MOD the described lag between the annual maximum temperature at the surface and the lower soil layers increases (cf. Figure 5-a)). This increased lag - and as Figure 3-b) shows an increase of available soil moisture with depth - an increase of differences in soil temperature is observed (cf. 5-b)). The difference in the 9th layer is smaller with values up to +/- 1 K and zero for the 10th layer (not shown) where the temperature is prescribed as a boundary value (cf. Section 2.1).

In contrast to the upper soil layers the lower levels show differences between both simulations during winter period as well. The higher heat capacity of wet soil leads not only to a decrease of the summer soil temperature by up to 2.5 K (cf. Figure 8-i) but also to a weaker cooling of the lower soil layers by 1.5 K in winter in MOD compared to CTL.

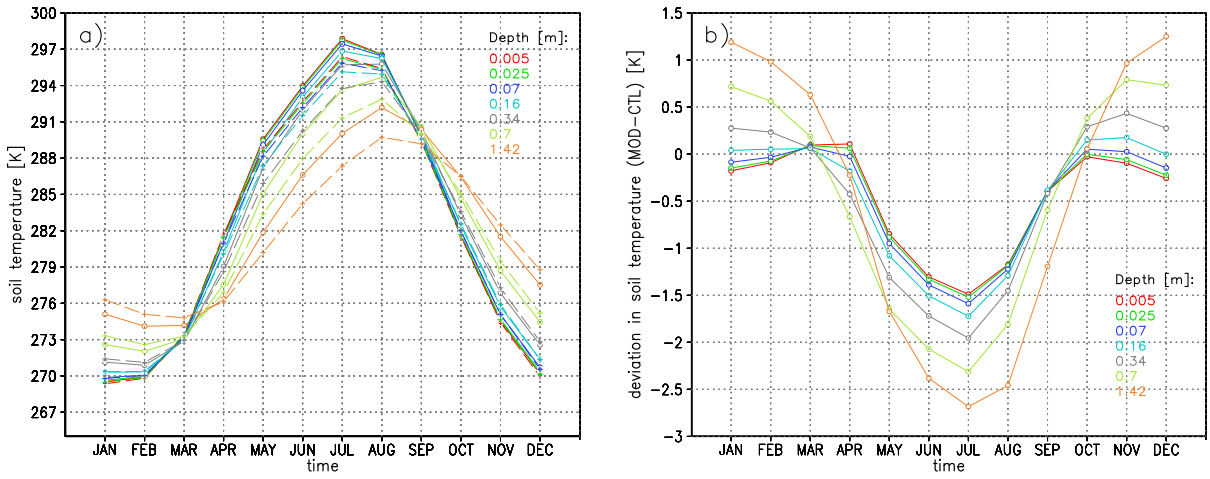

Fig. 5 Mean annual cycle of soil temperature for all soil layers affected by the roots a) for CTL simulation (solid) and MOD simulation (dashed) and b) as the difference between MOD and CTL as the relation MOD-CTL and as the mean over the connected silt loam area north of the Black Sea (cf. Figure 1). The numbers indicate the mean depth of each soil layer, measured from the earth's surface.

As a result of increasing latent heat flux, the Bowen Ratio (the ratio between energy available for sensible heating and energy available for latent heating) decreases (e.g. from 1 to 0.5 in July) (see Figure 4). This leads to an increase of water vapour concentration in the boundary layer (*Eltahir* (1998)) and also to an increase of backscattered terrestrial radiation in the atmosphere. This, in combination with a decrease of ground and surface temperature results in an increase of net terrestrial radiation at the surface by up to 6 W/m^2 in July and August (see Table 2 for exact values).

Between May and August increases of relative air humidity (of about 6 %) and of specific humidity (in July from $8.8*10^{-3}$ in the control simulation to $9.6*10^{-3}$ kg/kg in the modified simulation) are evident. As the mean total cloud cover between May and August is 0.5, the increase of the cloud cover in the MOD simulation by 10 % is small (cf. Figure 8-c)). Hence in this time the changes in net solar radiation are also of low magnitude of about -2.5 W/m^2 (cf. Table 2 and Figures 8-a) and -b)).

Compared to the CRU data, summer precipitation in the modified simulation is still underestimated. However, an increase of simulated precipitation for both, large scale and convective precipitation can be seen. Figure 2 shows the mean differences in precipitation summer (JJA) between the control and the modified simulations compared with CRU data for the period 1993-2002. In general, we find significant changes during

Table 2 Summary of CTL and MOD experiments: mean of the 13 years simulated for the month May, July and September. The values are spatial averages over the connected silt loam area north of the Black Sea (cf. Figure 1). SW net denotes net shortwave radiation, LW net is the net longwave radiation, NR net radiation, LH latent heat flux, SH sensible heat flux.

Fields	Units	May			July			September		
		CTL	MOD	Δ	CTL	MOD	Δ	CTL	MOD	Δ
Hydrological cycle										
- Precipitation	mm/day	1.02	1.10	+0.08	1.00	1.08	+0.08	1.02	1.02	+0.00
- Evaporation	mm/day	-1.70	-2.19	-0.49	-1.28	-2.08	-0.8	-0.56	-0.65	-0.09
- Runoff	mm/day	-0.14	-0.05	+0.06	-0.22	-0.12	+0.10	-0.18	-0.06	+0.12
- Soil moisture										
→ (upper 10cm)	mm	2.05	2.58	+0.53	1.90	2.33	+0.43	1.95	2.23	+0.28
	% of sat	46.0	53.3	+7.3	42.8	48.0	+7.2	43.7	46.0	+2.3
→ (root zone)	mm	26.59	39.68	+13.09	22.32	32.44	+10.12	21.63	29.60	+7.97
	% of sat	31.5	43.1	+11.6	26.4	35.2	+8.8	25.6	32.1	+6.5
→ (total)	mm	45.87	72.86	+26.99	41.52	59.84	+18.32	40.83	55.21	+14.37
	% of sat	46.0	53.3	+7.3	42.8	48.0	+7.2	43.7	46.0	+2.3
Surface energy budget										
- SW net	W/m^2	179.58	177.32	-2.26	187.24	184.93	-2.31	115.98	117.14	+1.16
- LW net	W/m^2	-75.30	-71.05	+4.25	-78.19	-71.21	+6.98	-73.67	-72.21	+1.46
- Net Radiation	W/m^2	104.28	106.27	+1.99	109.05	113.72	+4.67	42.31	44.93	+2.26
- SH	W/m^2	-43.02	-32.70	+10.37	-61.11	-43.58	+17.53	-29.60	-27.49	+2.11
- LH	W/m^2	-49.28	-63.41	-14.14	-37.09	-60.70	-23.61	-16.18	-18.75	-2.57

May-September over the southeast of Europe. In the area of interest the total precipitation in summer is increased by up to 10 %, in July for example from 1 mm/day in CTL to 1.08 mm/day in MOD (see Table 2 for May and September).

The mean temporal evolution of precipitation, evaporation and runoff as the spatial mean over the connected silt loam area north of the Black Sea (cf. Figure 1) is presented in Figure 6. From January to March and from September to December the precipitation rate is higher than the evaporation rate. As the soil layers are not at saturation the additional water can be stored in the soil. A part of this extra water is stored in snow. An increase of the soil moisture from September until April is observed (cf. Figure 7-a). From April onwards the increase of evaporation is substantial, while the rate is higher in the MOD simulation compared to CTL, due to the higher water storage especially in the spring time (cf. Figure 7-b). The evaporation increases in both simulations until June and decreases afterwards, due to the progress of the soil drying. Figure 8-f) presents the changes between MOD simulation and the CTL in summer mean sea level pressure. In the greater area of interest an decrease of surface pressure occurs of the order of -0.5-0 hPa.

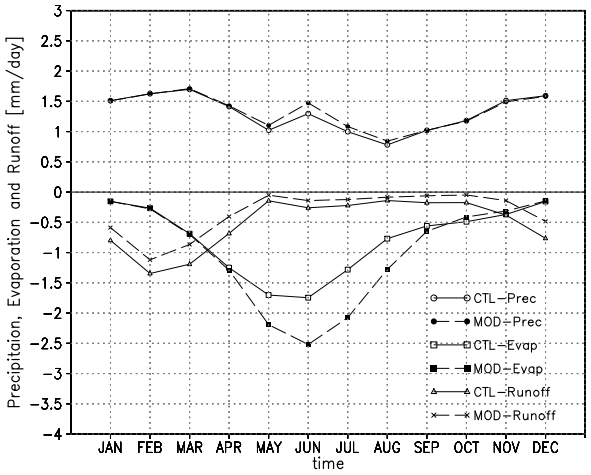

Fig. 6 Temporal evolution of precipitation (dots), evaporation (squares), and runoff (triangle,cross) over the connected silt loam area north of the Black Sea (cf. Figure 1) in the CTL (solid) and MOD (dashed) integrations in mm/day.

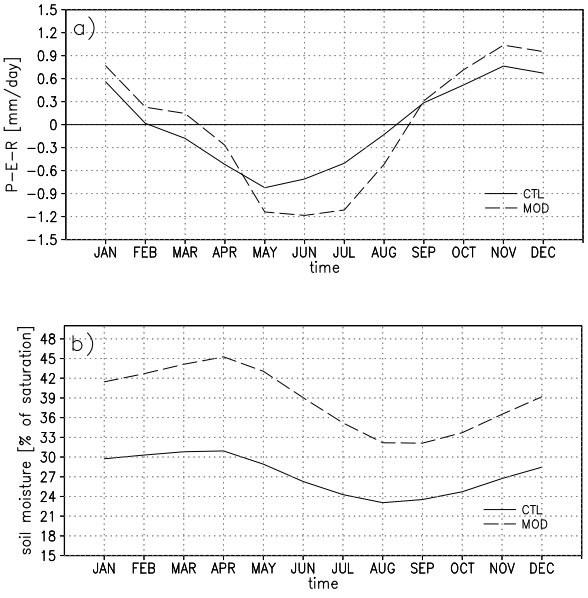

Fig. 7 Temporal evolution of the a) net input of water in the soil (precipitation-evaporation-runoff) in mm/day and b) the relative soil moisture content in the root zone in % of saturation. The values for CTL (solid) and MOD (dashed) integrations are spatially averaged over the connected silt loam area north of the Black Sea (cf. Figure 1) .

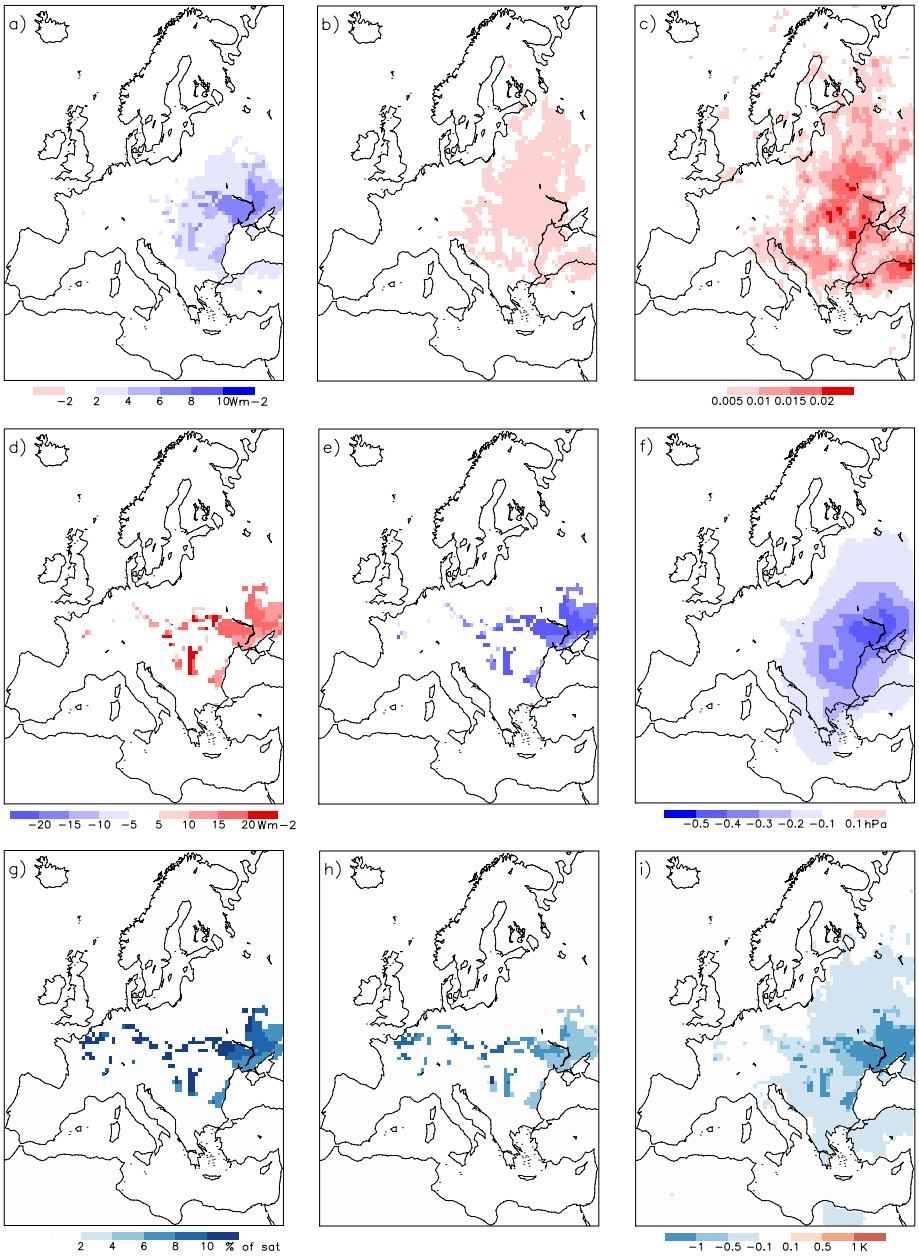

Fig. 8 Difference between both simulations (MOD-CTL) over the time period June-August (1993-2005) for a) net longwave radiation, b) net shortwave radiation, c) total cloud cover, d) sensible heat flux, e) latent heat flux, f) mean sea level pressure, g) soil moisture in the root zone, h) soil moisture in the upper 10cm, and i) temperature in the upper soil layer.

4 Conclusions

In a number of different RCM simulations dry and warm biases over south-eastern Europe have been observed. We test here the hypothesis that the biases are related to a false representation of soil properties in this region, based on divergences between the soil maps of *Haase et al.* (2007) and *Stremme* (1937) and that of FAO which is commonly used in (regional and global) climate models. Therefore we carried out two simulations with the RCM CLM using default sandy loam and silt loam over an area north of the Black Sea. Key results of this study are:
Due to its higher porosity, silt loam assimilates more water during rainfalls than sandy loam. This leads to a 30 % to 75 % increase in soil moisture in the modified simulation compared to the control simulation. The wet ground leads to a decrease of surface albedo and thus an increase of net solar radiation. The air temperature decreases by up to 1.5 K because more energy is needed for evaporation. During summer we have found a 60 % higher evaporation rate with increased humidity in air in the modified simulation compared to the control simulation. In the southeast of Europe the higher concentration of water within the boundary layer of the modified simulation causes more precipitation in the summer months. The study shows that heat fluxes and differences in soil moisture are limited to the silt loam area whereas radiation, total cloud cover and changes in mean sea level pressure also occur in a larger region.
We can conclude that using a silt loam distribution from the *International soil map of Europe* combined with the FAO soil map improves the models representation of the observed climate in the region with modified soil type. Nevertheless this modification fails to remove most of the model bias in south-eastern Europe, because the area where the modification is performed is only a small part of the region affected by the "summer drying" bias. We can nonetheless postulate based on our results that the specification of soil type is clearly important for such biases and may be relevant for other regions as well. It is a major contribution in reducing the phenomena of summer drying in the RCMs. Our results confirm that improving the simulation of processes within the boundary layer strongly depends on the improvement of the simulation of soil moisture.

Acknowledgements We would like to thank Danielle Hoja from German Aerospace Center for help to rectify the atlas map. The simulations have been performed at the German High Performance Computing Centre for Climate- and Earth System Research (DKRZ). Discussions with Jonas Bhend, Sebastian Wagner, Erich Fischer and Kerstin Proemmel were highly appreciated.

References

Betts, A. K. (2004), Understanding hydrometeorology using global models, *Bull Amer Meteorol Soc*, *85*(11), 1673–1688, doi:10.1175/BAMS-85-11-1673.

Betts, A. K., J. H. Ball, A. C. M. Beljaars, M. J. Miller, and P. A. Viterbo (1996), The land surface-atmosphere interaction: A review based on observational and global modeling perspectives, *J Geophys Res*, *101*(D3), 7209–7225.

Block, A. (2007), Unsicherheiten in Oberflächen- und Bodenparametern und ihre Auswirkungen auf die Ergebnisse regionaler Klimasimulationen, Ph.D. thesis, Brandenburgische Technische Universitt Cottbus.

Böhm, U., M. Kücken, W. Ahrens, A. Block, D. Hauffe, K. Keuler, B. Rockel, and A. Will (2006), CLM - the climate version of LM: Brief description and long-term applications, *COSMO Newsletter*, *6*, 225–235.

Christensen, J. H., B. Machenhauer, R. G. Jones, C. Schär, P. M. Ruti, M. Castro, and G. Visconti (1997), Validation of present-day regional climate simulations over Europe: LAM simulations with observed boundary conditions, *Clim Dyn*, *13*(7-8), 489–506.

Davies, H. (1976), A lateral boundary formulation for multi-level prediction models, *Quart J Roy Meteor Soc*, *102*, 405–418.

Dickinson, R. (1984), Modeling evaporation fior three-dimensional global climate models, in *Climate processes and climate sensitivity*, *Geophysical Monograph*, vol. 29, edited by J. Hansen and T. Takahashi, pp. 58–72, American Geophysical Union.

Dickinson, R., A. Henderson-Sellers, P. Kennedy, and M. Wilson (1986), Biosphere-atmosphere transfer scheme (bats) forcing the ncar community climate model, *NCAR Technical Note TN275+STR*, NCAR.

Doms, G., J. Förstner, E. Heise, H.-J. Herzog, M. Raschendorfer, R. Schrodin, T. Reinhardt, and G. Vogel (2002), A description of the nonhydrostatic regional model LM, Part II: physical parametrization, *Tech. rep.*, Deutscher Wetterdienst, Offenbach.

Driessen, P. (1986), The water balance of soil, in *Modelling of agriculteral production: weather, soils and crops*, edited by H. Van Keulen and J. Wolf, pp. 76–116, Poduc.

Eltahir, E. A. B. (1998), A soil moisture rainfall feedback mechanism 1. Theory and observations, *Water Resour Res*, *34*(4), 765–776.

FAO (1996), The digitized soil map of the World including derived soil properties, *Food and Agriculture Organization, Rom.*

FAO/UNESCO (1974), *Soil Map of the World*, UNESCO.

Fennessy, M. J., and J. Shukla (1999), Impact of initial soil wetness on seasonal atmospheric prediction, *J Clim*, *12*(11), 3167–3180.

Ferranti, L., and P. Viterbo (2006), The european summer of 2003: Sensitivity to soil water initial conditions, *J Clim*, *19*(15), 3659–3680.

Feser, F., and H. von Storch (2005), A spatial two-dimensional discrete filter for limited-area-model evaluation purposes, *Mon Weather Rev*, *133*(6), 1774–1786.

Findell, K. L., and E. A. B. Eltahir (2003a), Atmospheric controls on soil moisture-boundary layer interactions. Part I: Framework development, *J Hydrometeor*, *4*(3), 552–569.

Findell, K. L., and E. A. B. Eltahir (2003b), Atmospheric controls on soil moisture-boundary layer interactions. Part II: Feedbacks within the continental United States, *J Hydrometeor*, *4*(3), 570–583.

Fischer, E. M., S. I. Seneviratne, D. Lüthi, and C. Schär (2007a), Contribution of land-atmosphere coupling to recent European summer heat waves, *Geophys Res Lett*, *34*(6), doi:10.1029/2006GL029068.

Fischer, E. M., S. I. Seneviratne, P. L. Vidale, D. Lüthi, and C. Schär (2007b), Soil moisture - atmosphere interactions during the 2003 European summer heat wave, *J Clim*, *20*, 5081–5099, doi:10.1175/JCLI4288.1.

Haase, D., J. Fink, G. Haase, R. Ruske, M. Pecsi, H. Richter, M. Altermann, and K. D. Jager (2007), Loess in Europe - its spatial distribution based on a European loess map, scale 1 : 2,500,000, *Quat Sci Rev*, *26*(9-10), 1301–1312.

Hagemann, S., M. Botzet, and B. Machenhauer (2001), The summer drying problem over south-eastern Europe: Sensitivity of the limited area model HIRHAM4 to improvements in physical parameterization and resolution, *Physics and Chemistry of*

the Earth, Part B, *26*(5-6), 391–396.

Hagemann, S., B. Machenhauer, R. Jones, O. B. Christensen, M. Déqué, D. Jacob, and P. L. Vidale (2004), Evaluation of water and energy budgets in regional climate models applied over Europe, *Clim Dyn*, *23*(5), 547–567, doi:10.1007/s00382-004-0444-7.

Jacob, D., et al. (2007), An inter-comparison of regional climate models for Europe: model performance in present-day climate, *Clim Change*, *81*, 31–52.

Jaeger, E. B., I. Anders, D. Lüthi, B. Rockel, C. Schär, and S. I. Seneviratne (2008), Analysis of era40-driven clm simulations for europe, *Meteorol Z*, *17*(4), 349–367.

Kalnay, E., et al. (1996), The ncep/ncar 40-year reanalysis project, *Bull Amer Meteorol Soc*, *77*(3), 437–471.

Koster, R. D., and M. J. Suarez (2001), Soil moisture memory in climate models, *J Hydrometeor*, *2*(6), 558–570.

Koster, R. D., and M. J. Suarez (2003), Impact of land surface initialization on seasonal precipitation and temperature prediction, *J Hydrometeor*, *4*(2), 408–423.

Koster, R. D., et al. (2004), Regions of strong coupling between soil moisture and precipitation, *Science*, *305*(5687), 1138–1140.

Koster, R. D., et al. (2006), Glace: The global land-atmosphere coupling experiment. part i: Overview, *J Hydrometeor*, *7*(4), 590–610, doi:10.1175/JHM511.1.

Machenhauer, B., M. Windelband, M. Botzet, J. Christensen, D. M., R. Jones, P. Ruti, and G. Visconti (1998), Validation and analysis of regional present-day climate and climate change simulations over Europe, *Report 275*, Max-Planck-Institute for Meteorology.

Marshall, C. H., R. A. Pielke, L. T. Steyaert, and D. A. Willard (2004), The impact of anthropogenic land-cover change on the florida peninsula sea breezes and warm season sensible weather, *Mon Weather Rev*, *132*(1), 28–52.

Mitchell, T. D., and P. D. Jones (2005), An improved method of constructing a database of monthly climate observations and associated high-resolution grids, *Int J Climatol*, *25*(6), 693–712.

Moberg, A., and P. D. Jones (2004), Regional climate model simulations of daily maximum and minimum near-surface temperatures across Europe compared with observed station data 1961-1990, *Clim Dyn*, *23*(7-8), 695–715.

Noguer, M., R. Jones, and J. Murphy (1998), Sources of systematic errors in the climatology of a regional climate model over Europe, *Clim Dyn*, *14*(10), 691–712.

Pan, Z. T., R. W. Arritt, W. J. Gutowski, and E. S. Takle (2001), Soil moisture in a regional climate model: simulation and projection, *Geophys Res Lett*, *28*(15), 2947–2950.

Pielke, R. A. (2001), Influence of the spatial distribution of vegetation and soils on the prediction of cumulus convective rainfall, *Rev Geophys*, *39*(2), 151–177.

Pielke, R. A., R. L. Walko, L. T. Steyaert, P. L. Vidale, G. E. Liston, W. A. Lyons, and T. N. Chase (1999), The influence of anthropogenic landscape changes on weather in south Florida, *Mon Weather Rev*, *127*(7), 1663–1673.

Räisänen, J., U. Hansson, A. Ullerstig, R. Doscher, L. P. Graham, C. Jones, H. E. M. Meier, P. Samuelsson, and U. Willen (2004), European climate in the late twenty-first century: regional simulations with two driving global models and two forcing scenarios, *Clim Dyn*, *22*(1), 13–31.

Rowell, D. P., and R. G. Jones (2006), Causes and uncertainty of future summer drying over Europe, *Clim Dyn*, *27*(2-3), 281–299.

Sánchez, E., M. A. Gaertner, C. Gallardo, E. Padorno, A. Arribas, and M. Castro (2007), Impacts of a change in vegetation description on simulated European summer present-day and future climates, *Clim Dyn*, *29*(2-3), 319–332.

Schär, C., D. Lüthi, U. Beyerle, and E. Heise (1999), The soil-precipitation feedback: Area process study with a regional climate model, *J Clim*, *12*(3), 722–741.

Schrodin, R., and E. Heise (2001), The multi-layer version of the DWD soil model TERRA-LM, *COSMO Technical Report 2*, Deutscher Wetterdienst.

Seneviratne, S. I., D. Lüthi, M. Litschi, and C. Schär (2006a), Land-atmosphere coupling and climate change in europe, *Nature*, *443*(7108), 205–209, doi: 10.1038/nature05095.

Seneviratne, S. I., et al. (2006b), Soil moisture memory in AGCM simulations: Analysis of global land-atmosphere coupling experiment (GLACE) data, *J Hydrometeor*, *7*, 1090–1112.

Stremme, H. (1937), International soil map of Europe, 1:2500000, *Gea Verlag, Berlin*.

Teuling, A., and S. I. Seneviratne (2008), Contrasting spectral changes limit albedo impact on land-atmosphere coupling during the 2003 european heat wave, *Geophys Res Lett*, *35*, L03,401, doi:10.1029/2007GL032778.

Vidale, P. L., D. Lüthi, C. Frei, S. I. Seneviratne, and C. Schär (2003), Predictability and uncertainty in a regional climate model, *J Geophys Res*, *108*(D18), 4586.

Wu, W. R., and R. E. Dickinson (2004), Time scales of layered soil moisture memory in the context of land-atmosphere interaction, *J Clim*, *17*(14), 2752–2764.

Zaitchik, B. F., J. P. Evans, R. A. Geerken, and R. B. Smith (2007), Climate and vegetation in the middle east: Interannual variability and drought feedbacks, *J Clim*, *20*(15), 3924–3941, doi:10.1175/JCLI4223.1.